Modelling of Flame Acceleration due to Intrinsic Instabilities in Industrial Scale Explosions

Helene H. Pedersen[a,b]
Prankul Middha[a]
Trygve Skjold[a,b]
Kees van Wingerden[a]
Bjørn J. Arntzen[a,b]

[a]GexCon AS, Bergen, Norway
[b]University of Bergen, Department of Physics and Technology, Bergen, Norway

1 Introduction

Modelling of explosions using Computational Fluid Dynamics (CFD) is useful for performing risk assessments in the petrochemical industries that handle flammable gases and liquids. In order to represent large-scale explosions in complex geometries, subgrid models for e.g. combustion and turbulence are necessary. In the CFD-tool FLACS [1], the accelerating effect of flame instabilities during the early phase of flame propagation is modelled by an empirical equation that controls the effective burning velocity during the transition from laminar to fully turbulent flow regimes. Recent validation work suggests that it is necessary to review and improve this model in light of the experimental and analytical efforts that have been made on the subject since its implementation.

The present work focuses on the instabilities associated with the combustion process itself. These *intrinsic* instabilities would occur even if there were no surroundings for the flame to interact with [2], and will therefore often dominate the early phase of combustion. In contrast, when obstructions and confinement are present, other mechanisms, such as the *Kelvin-Helmholtz* and *Rayleigh-Taylor* instabilities, will dominate. In closed vessels and ducts, acoustic waves created by the flame can lead to various instability phenomena, as pointed out by e.g. Ciccarelli and Dorofeev [3]. However, if the initial flame is allowed to expand freely for a while, acceleration due to intrinsic instabilities can have a significant effect on the later development. This situation is especially relevant for large scale geometries.

2 Mechanisms of intrinsic flame instabilities

Darrieus [4] and Landau [5] found that a freely propagating laminar flame resulting from a weak ignition source is unconditionally unstable, due to the expansion of the gas through the flame. The transition

Correspondence to: helene@gexcon.com

between the stable and unstable propagation of a spherical flame is marked by the appearance of a structured, cellular surface at a specific radius, given by the critical *Peclet number*

$$Pe = \frac{R_F}{\delta_L} ,$$

where R_F is the flame radius, and δ_L is the laminar flame thickness [3]. See Figure 1 for an illustration.

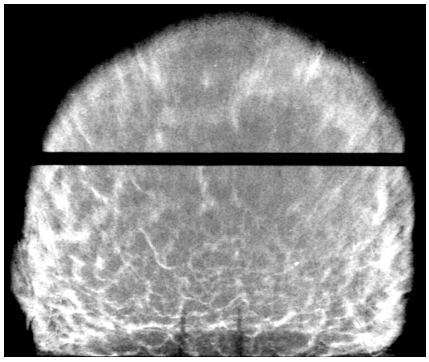

Figure 1: A flame ball with the cellular structure that is characteristic for unstable propagation, from an experiment performed at CMR [6].

According to Bechtold and Matalon [7], the critical Peclet number is dependent on the *Lewis number* (the ratio of the thermal diffusion to the mass diffusion) and the activation energy, for a given expansion ratio. These effects can be combined by introducing the *Markstein number*, Ma, as described by Bradley [8]. Ma is defined as the *Markstein length* L_M, normalised by the flame thickness δ_L, where L_M measures the effect of curvature on the burning velocity. The effects of stretch on the laminar burning velocity can be expressed as

$$\frac{S_L - S_N}{S_L} = KMa ,$$

where S_L is the laminar burning velocity, S_N is the burning velocity at a given stretch rate, and

$$K = \frac{1}{A}\frac{dA}{dt}\frac{\delta_L}{S_L}$$

is the *Karlovich stretch rate*. Here, A is the area of the flame.

During the early stages of flame propagation, when the flame stretch rate is high, the hydrodynamic instability can be counteracted by thermal-diffusive effects. For small, and especially negative Markstein numbers, the thermal-diffusive effects will enhance the hydrodynamic instabilities. As a consequence, the flame will exhibit unstable behaviour almost from the moment of ignition. Therefore, rich hydrocarbon flames (characterised by small Markstein numbers) will behave quite differently from lean hydrocarbon flames. The intrinsic instabilities will eventually lead to a turbulent regime, marked by a considerable increase in flame speed due to the subsequent wrinkling of the flame [8].

3 Relevant experiments

This section reviews selected experiments involving intrinsic instabilities. A report of Lind and Whitson [9] describes a series of experiments with balloons of radii 5 and 10 m for near-stoichiometric

mixtures of methane, propane, ethylene, ethylene oxide, butadiene and acetylene mixed with air. The development of the flame radius in time, determined from video recordings, is reported.

The work of van Wingerden *et al.* [10] describes the flame propagation in initially quiescent near-stoichiometric mixtures of methane, propane, ethane, and combinations of these with air. The experiments were conducted in a 5 m $\times$ 5 m $\times$ 2.5 m tent, and the flame propagation was monitored using ionization gaps. The results reviewed here are from two tests with a 9.8 $\%$ methane-air mixture and a 4.2 $\%$ propane-air mixture, ignited centrally. Only the initial phase of combustion was studied – up to a flame radius of about 1-2 m. The results are corrected for the buoyancy effects by simple calculation, assuming a perfectly spherical flame ball and vertical displacement in time only.

The development of the flame radius for the experiments is shown in Figure 2. The CMR [10] results for the initial laminar combustion phase of methane and propane seem to agree well with the results of the larger experiments reported by Lind and Whitson [9]. Nearly all of the experiments were performed with near-stoichiometric mixtures, except for one rich propane (5%) test [9].

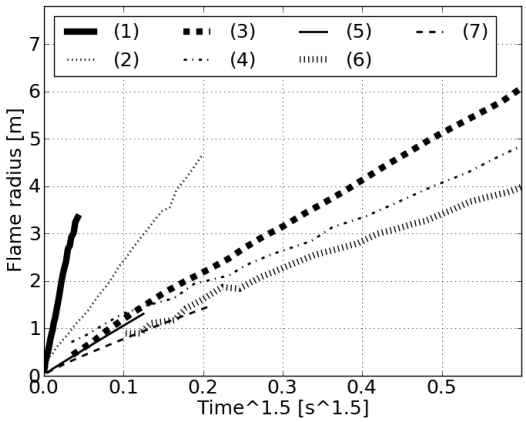

Figure 2: (1) Acetylene 7.7% [9] (2) Ethylene 6.5% [9] (3) Propane 5% [9] (4) Propane 4% [9] (5) Propane 4.2 % [10] (6) Methane 10% [9] (7) Methane 9.8 % [10]

4 Modelling of flame acceleration due to intrinsic instabilities

Flame acceleration due to intrinsic instabilities is modelled in FLACS by introducing a quasi-laminar burning velocity S_{QL} for the initial phase, since the numerical flame is too thick to resolve the flame front, including wrinkling effects [1].

$$S_{QL} = S_L \left(1 + a \sqrt{\min \left(1, \frac{R_F}{3} \right)} \right) \ , \tag{1}$$

where a is an empirical constant specific to the type of gas. The expression in (1) was derived from validation against experimental data. Markstein number effects are presently not included in the model, at least not explicitly, implying that concentration effects are not taken into account. Observe that the submodel for the quasi-laminar burning velocity is only active up to a flame radius of 3 m.

Gostintsev *et al.* [11] have presented an analysis of a number of experiments, including the ones described by Lind and Whitson in [9]. They demonstrated the existence of a self-similar turbulent regime

of flame propagation, which develops at a certain critical flame radius. The expression for the flame radius for a freely propagating spherical flame is given as

$$R_F = R_1 + Ct^{\frac{3}{2}} \ . \tag{2}$$

The empirical constants R_1 and C can be derived from Figure 2. An expression for the flame speed V_F follows directly from (2)

$$V_F = \frac{\partial R_F}{\partial t} = \frac{3}{2} C t^{\frac{1}{2}} = \frac{3}{2} C^{\frac{2}{3}} (R_F - R_1)^{\frac{1}{3}} \ . \tag{3}$$

For an outwardly propagating flame, the burning velocity is given by $\sigma S_{QL} = V_F$, where σ is the expansion rate, and hence

$$S_{QL}(R_F) = \frac{3}{2} \frac{C^{\frac{2}{3}}}{\sigma} (R_F - R_1)^{\frac{1}{3}} \ . \tag{4}$$

In Figure 2 the experimental flame radius measurements are plotted against $t^{\frac{3}{2}}$. The results are in agreement with the observations of Gostintsev *et al.* [11]. Expressions (1) and (4) for the quasi-laminar burning velocity from two of the propane experiments are plotted in Figure 3. Here, the expression of Gostintsev *et al.* [11] predicts smaller burning velocities for a 4% propane mixture than the FLACS formulation does. For the richer 5 % propane mixture, we have the opposite situation.

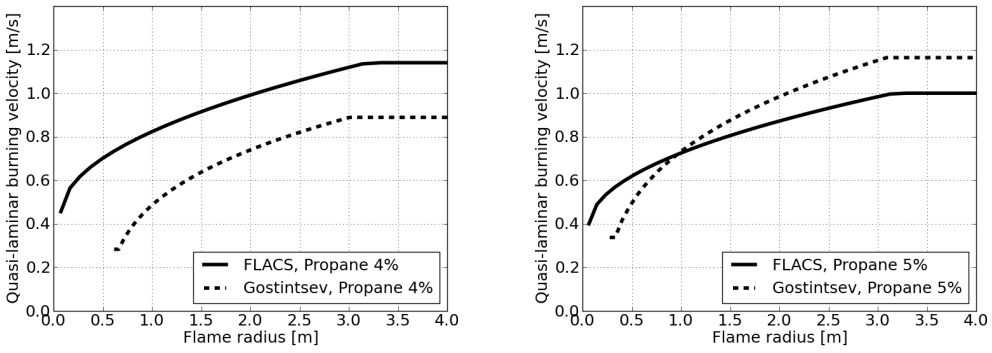

(a) (b)

Figure 3: Comparison of the quasi-laminar burning velocity in FLACS [1] and the expression from Gostintsev *et al.* [11].

5 Model results

The CFD tool FLACS was used to simulate selected scenarios from the experiments presented above. Different grid resolutions were used, to uncover grid dependency problems. The results for methane and propane mixtures with air are included here.

The simulated flame radii for methane are very close to the experimental values, see Figure 4(a). Lind and Whitson [9] reported a flame velocity of 7.3 m/s at 3 m and 8.9 m/s at 8 m in the vertical direction. FLACS deviates less than 10% for flame radii exceeding 8 m, which must be considered to be well within the uncertainty of the experimental measurements. For propane (Figure 4(b)), FLACS overpredicts the velocity in the initial phase. At 8 m, however, the agreement seems to be satisfactory.

The simulations of the CMR experiments [10] indicate that the initial flame acceleration is too large in FLACS for the coarser grids, see Figure 5. The difference between methane and propane is less pronounced here. Simulations with constant burning velocities indicate that much of the grid sensitivity originates from the flame model in FLACS.

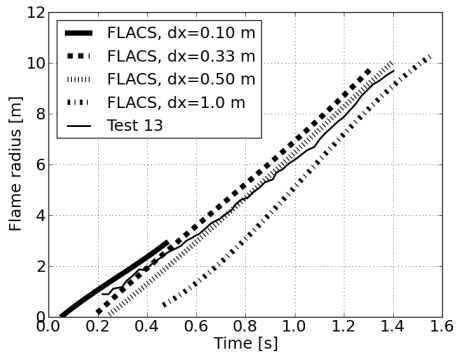

(a) Methane 10%

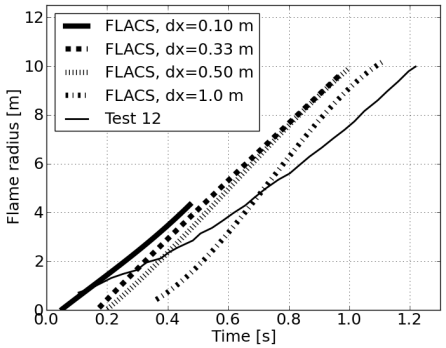

(b) Propane 4%

Figure 4: Flame radius data for 10 m radius hemispherical balloon test [9], together with FLACS results for various grid resolutions.

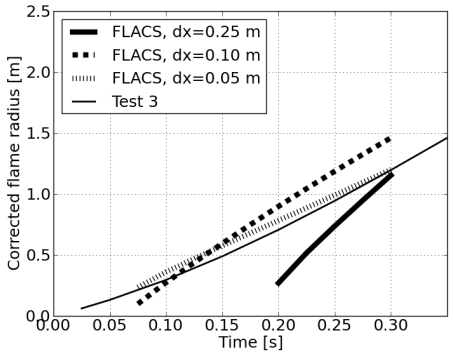

(a) Methane 9.8 %

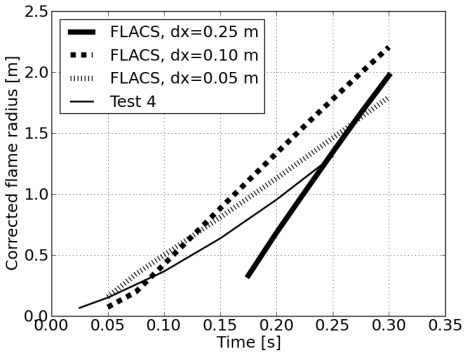

(b) Propane 4.2%

Figure 5: Flame radius data for a 62.5 m^3 tent [10], together with FLACS results for two grid resolutions.

6 Final remarks

The plotted data from van Wingerden *et al.* [10] are corrected for the upward movement of the flame ball due to buoyancy effects, while the data from Lind and Whitson [9] are not. Since Lind and Whitson [9] attribute some of the acceleration observed in the vertical direction to buoyancy, the contribution of the hydrodynamic instabilities is not clear. However, simulations in FLACS suggest that the buoyancy has a limited effect on the shape of the the flame radius vs. time curves. Experimental measurements of flame speed as a function of distance to ignition point are quite sensitive to variations in initial conditions [10], and turbulence production at the time of ignition can affect the results considerably.

In general, it is a challenge to test how the model responds to the occurence of intrinsic instabilities, when the majority of the experiments concerns stoichiometric mixtures. As a consequence, the analysis of Gostintsev *et al.* [11] may not apply to low Markstein number mixtures, such as lean hydrogen or rich hydrocarbon flames. The comparison between the burning velocities in Figure 3 shows that the formulation in (4) will yield lower values for 4% propane mixtures, as desired in the validation study of Section 5, while it will enhance the burning in a richer mixture more prone to instabilities. It is however challenging to ensure that the right mechanisms are taken care of in other cases, where the experimental conditions used to create this expression does no longer apply. A more fundamental study is therefore

needed, where a wide range of gases and concentrations are investigated, also for large scales.

7 Conclusions

1. The results from the CMR 62.5 m^3 [10] tent experiments agree well with the other results from literature considered here.
2. The effect of flame instabilities on the flame acceleration is clear from the experiments, and seems to be well described by the analysis of Gostintsev *et al.* [11] for near-stoichiometric mixtures.
3. While FLACS seems to predict the flame velocity at large flame radii well, the comparison between simulations and experiments indicates that a model that takes into account the Markstein number effects during the initial phase should be considered.
4. The validation study should be extended to other gases, especially other mixtures. Hence, there is a strong need for high-quality experimental data with a greater variety of gases and concentration.

References

[1] Arntzen, B. J. (1998). Modelling of turbulence and combustion for simulation of gas explosions in complex geometries. Doctoral thesis NTNU. 1998: 120

[2] Matalon, M. (2007). Intrinsic flame instabilities in premixed and nonpremixed combustion. Annual Review of Fluid Mechanics. 39: 163-191

[3] Ciccarelli, G. and Dorofeev, S. (2008). Flame acceleration and transition to detonation in ducts. Progress in Energy and Combustion Science. 34: 499-550

[4] Darrieus, G. (1938). Propagation d'un front de flamme. Presented at La Technique Moderne (Paris) and in 1945 at Congrès de Méchanique Appliquée (Paris)

[5] Landau, L. D. (1944). On the theory of slow combustion. Acta Physicochim. USSR. 19: 77-85

[6] Wilkins, B. A. and van Wingerden, K. (1994). The influence of waterspray on quasi-laminar combustion. Christian Michelsen Research. Report No. CMR-94-F25006

[7] Bechtold, J. K. and Matalon, M. (1987). Hydrodynamic and diffusion effects on the stability of spherically expanding flames. Combustion and Flame. 67: 77-90

[8] Bradley, D. (1999). Instabilities and flame speeds in large-scale premixed gaseous explosions. Philosophical Transactions: Mathematical, Physical and Engineering Sciences. 357: 3567-3581

[9] Lind, C. D. and Whitson, J. C. (1977). Explosion hazards associated with spills of large quantities of hazardous materials: Phase 2. Department of transportation, United States Coast Guard. Report No. CG-D-85-77

[10] van Wingerden, K., Wilkins, B. A., and Pedersen, G. H. (1994). Large scale laminar combustion tests. Christian Michelsen Research. Report No. CMR-94-F25064

[11] Gostintsev, Yu. A., Istranov, A. G., and Shulenin, Yu. V. (1989). Self-similar propagation of a free turbulent flame in mixed gas mixtures. Combustion, Explosion, and Shock Waves. 24: 563-569